Radioluminescence and Optically Stimulated Luminescence Responses of a Cerium-Doped Sol-Gel Silica Glass Under X-Ray Beam Irradiation

Nissrine Al Helou, Hicham El Hamzaoui, B. Capoen, Géraud Bouwmans, Andy Cassez, Y. Ouerdane, A. Boukenter, Sylvain Girard, G. Chadeyron, Rachid Mahiou, et al.

Radioluminescence and Optically Stimulated Luminescence Responses of a Cerium-doped Sol-gel Silica Glass under X-ray Beam Irradiation

N. Al Helou, H. El Hamzaoui, B. Capoen, G. Bouwmans, A. Cassez, Y. Ouerdane, A. Boukenter, S. Girard, *Senior Member IEEE*, G. Chadeyron, R. Mahiou and M. Bouazaoui.

Abstract— **Ce-doped sol-gel silica glasses were prepared for real-time X-ray dose or dose rate monitoring using radioluminescence (RL) and optically stimulated luminescence (OSL). A small piece of this glass scintillator was connected to two optical fibers, allowing a remote measurement of the ionizing radiation dose through RL and OSL signals. By using this Ce-doped material, we particularly demonstrated that the RL signal shows a linear behavior at least up to dose rates of 1.2 Gy/s. Furthermore, the linear dose response of the OSL signal can be extended up to 500 Gy, independently of the used dose rate.**

Index Terms— **dosimetry, X-radiation, optical fibers, cerium, radioluminescence, optically stimulated luminescence.**

I. Introduction

During the last decades, a persistent and continuous work has been carried out to develop a convenient sensor enabling real-time sensing of radiations in harsh environment [1]-[3]. The optical fiber-based dosimetry could be a promising alternative to electronic dosimeters, due to its specific characteristics, such as its unique capability to perform remote and real-time monitoring, or its insensitivity to electromagnetic interferences. Furthermore, optical fibers having a small footprint and a low mass do not introduce large disturbances to the radiation field. For in vivo dosimetry applications, when using radiation as a curative tool, the prescribed and definitive dose should only be delivered to the organ of interest while restricting the dose absorbed by the surrounding healthy cells. Small dosimeters based on optical fibers have been used in radiotherapy treatments and radiodiagnostics to control the dose deposited on the patients [4]-[6]. These detectors are also interesting for difficult-to-access and hazardous regions like in nuclear reactors. It can be used in nuclear power plants to control nuclear activities, for protection of workers, in recycling and dismantling operations, in long-term nuclear storage and industrial process controls [7]. Moreover, the space environment is not as safe as the Earth's surface. It is characterized by a mixture of charged particles (Galactic cosmic rays: GCR), particles trapped by the planet magnetic field and their interactions with other species generate secondary particles, making the environment very complex. Aircrews, space-crews, but also frequent flyer passengers are often exposed to radiations, even in the atmosphere [8, 9]. Measurements using OSL dosimeters in unmanned satellites and shuttles could be a clever and innovative approach to monitor the space radiations [10], [11]. These detectors should be very sensitive in a large dose range. They should have a fast readout capability and should be economically suitable [1]. When high dose levels are expected, dosimeters encounter a new challenge concerning their response and their reproducibility.

Optically stimulated luminescence (OSL) is a recently developed passive method in dosimetry of ionizing radiation. This is a useful and important technique in order to get rid of the spurious light encountered while measuring radiation dose using a scintillation signal, the so-called "stem effects" (as Cerenkov radiation and defects emission in fiber optics). OSL fundamental mechanisms are almost the same as thermoluminescence (TL), except that the recombination of the trapped charges is stimulated by light with a proper probe wavelength, instead of heat. Thus, thermal quenching of the luminescence efficiency, which limits the TL sensitivity of the material, could be entirely avoided [9]. Firstly used as TL material, carbon-doped aluminum oxide (Al_2O_3:C) provides highly sensitive OSL dosimeters and can be potentially used in radiotherapy applications [12], [13] or for environmental

Manuscript received November 23, 2017. This work has been partially founded by the Agence Nationale de la Recherche through the LABEX CEMPI (ANR-11-LABX-0007) and the Equipex Flux (ANR-11-EQPX-0017), as well as by the Ministry of Higher Education and Research, Hauts-de-France Regional Council and European Regional Development Fund (ERDF) through the Contrat de Projets Etat-Region (CPER Photonics for Society P4S).

N. Al Helou, H. El Hamzaoui, B. Capoen, G. Bouwmans, A. Cassez and M. Bouazaoui are with PhLAM Laboratory, Université de Lille, F-59000 Lille, France (e-mail: nissrine.alhelou@ed.univ-lille1.fr).
Y. Ouerdane, A. Boukenter, and S. Girard are with Univ Lyon, Lab. Hubert Curien, CNRS UMR 5516, F-42000 Saint-Etienne, France.
G. Chadeyron and R. Mahiou are with Institut de Chimie de Clermont-Ferrand, Université Clermont Auvergne, F-63171 Aubièren, France.

monitoring (near nuclear waste storage facilities) [14]. However, this material shows a long luminescence lifetime (≈ 35 ms) and it takes a few minutes to read the entire signal. This constraint limits the possibility of applying the OSL of Al_2O_3:C for real-time radiotherapy dosimetry [14]. On the contrary, KBr:Eu crystal exhibits a short photostimulated luminescence lifetime (τ = 1.6 μs) which makes it a good candidate for use as a real-time OSL dosimeter [15], but it was found that the OSL sensitivity depends on radiation exposure time [16].

Cerium, an extremely favorable and stable scintillator dopant, is of great interest for dosimetry, especially in terms of radiation hardening. Besides its cerous trivalent state (Ce^{3+}), cerium can be found in its ceric tetravalent state (Ce^{4+}), but only Ce^{3+} leads to an efficient optical activity, due to the 4f–5d transition that may be exploited for radiation dosimetry. Radioluminescence (RL) of Ce-doped glasses has been widely reported in the literature. Studies on TL and OSL properties of Ce^{3+} ions are scarcer and mainly concern doped crystals. For example, an OSL response of a cerium-doped lutetium orthosilicate crystal has been found linear in the range 100 μGy - 1 Gy [17]. Another example concerns polycrystalline $CaSiO_3$:Ce phosphors prepared by solid state diffusion [18], where the OSL response was linear in the 20 - 20,000 mGy range. The OSL sensitivity of this latter material was 2.8 times that of Al_2O_3:C phosphors. However, these dosimeter crystals could not be drawn into optical fibers, which hinders their use in the targeted all-fibered integrated dosimetry devices. Glassy materials can overcome this drawback.

In general, photoluminescence (PL) spectra of a cerium-doped glass under UV excitation show a broad emission maximum located in the 375 and 460 nm spectral domain, depending on the glass composition and on its synthesis method. This band is assigned to the 4f-5d transition of Ce^{3+} ions [19]-[25]. The importance of inert [20] or reducing atmospheres [26]-[28] during glass synthesis has been demonstrated to favor the cerous state. Evaluating the response of Ce^{3+}-doped $CaO–Al_2O_3–B_2O_3$ glasses exposed to X-rays, linearity of TL and OSL signals was observed in 1–1000 mGy and 30–3000 mGy dose ranges, respectively [19]. Nevertheless, owing to the formation of defects in multicomponent glass under ionizing radiation, the use of Ce-doped pure silica glasses is of interest because of the well-known hardness of silica matrix. Hence, recent investigations of the RL response of a Ce^{3+}-doped SiO_2 detector, coupled to a passive fiber for dose measurements in ^{192}Ir HDR brachytherapy, revealed this setup as a promising miniaturized dosimeter [29].

Chiodini et al. [30] showed that a Ce-doped fiber dosimeter prototype exhibits a linear response up to 10 Gy under 6 MV photon beam. The RL response of the same fibered sample also undergoes linear and reproducible dose dependence under ^{60}Co γ-ray exposures up to 3.5 Gy, as well as an encouraging linear response under 38 MeV proton irradiation. Almost no published work deals with OSL studies in Ce-doped pure silica glass. Very recently, however, a linear response of the OSL and TL signals from 1 mGy to 2 Gy has been recorded using a Ce^{3+}-doped SiO_2 glass synthetized by a spark plasma sintering technique [31].

In the present work, to extend the use of Ce-doped materials to X-ray dosimetry in larger dose ranges, we investigate the potential of a Ce^{3+}-doped silica glass, prepared with the sol-gel process, as a remote radiation dosimeter based on RL and OSL responses. The sensor is based on a doped glass rod connected at both ends to a passive optical fiber used as a light guide toward the detector and toward the OSL excitation source. The aim is to study the linearity of the RL response at lower dose rates than in Ref. [20] and to investigate the OSL response at higher cumulative doses compared to the ones explored in previous studies. We also studied the post-irradiation fading of the OSL signal.

II. Materials and Methods

A. Investigated samples

Samples of ionic cerium-doped glassy rods were synthetized by the sol-gel technique from tetraethylorthosilicate (TEOS) precursor [32]. The obtained xerogels were stabilized at 1000°C and then soaked in alcoholic solution containing a cerium salt. After that, the samples were withdrawn from the doping solution and dried at 50°C for 24 hours in order to remove solvents and to retain cerium element within the nanopores. The doped matrices were then densified in helium atmosphere at 1200°C for 2 hours in order to obtain a higher Ce^{3+}/Ce^{4+} ratio and then to enhance the PL efficiency. The Ce-doped rod glass was jacketed with a pure silica tube and drawn at a temperature of about 2000°C down to a millimeter-sized cane. Electron probe micro-analysis (EPMA) shows a Ce concentration of about 0.07 wt% in the obtained sample. Furthermore, a molar concentration ratio $[Ce^{3+}]/[Ce^{4+}]$ of about 5 has been estimated for this sample, as it has been detailed in [20].

B. RL and OSL Experimental Setup

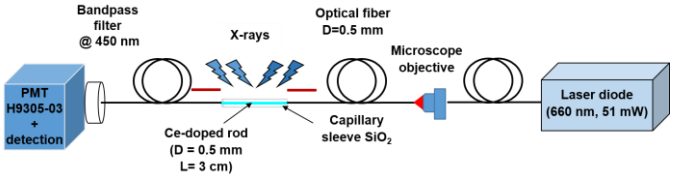

Fig. 1: Schematic illustration of the experimental setup used to characterize the OSL response of the fiber material exposed to X-ray beam.

For OSL measurements, the experimental setup was composed of a 3 cm-long piece of the doped rod, which was polished at both ends and then inserted in a pure silica sleeve. At both ends of this rod, a 0.5 mm diameter multimode pure silica core optical fiber was connected (Fig. 1). One of these fibers was used to guide the OSL signal toward a photomultiplier (PMT, H9305-03 Hamamatsu). The electrical signal provided by the PMT is read through a 500 MHz Tektronix oscilloscope that convert the luminescence signal into a voltage signal. A bandpass spectral filter at 450 ± 40 nm was chosen in order to select the OSL signal and eliminate the stimulating light of the laser diode at 660 nm. The other fiber was devoted to guide the stimulation light to the doped glassy rod while evaluating the OSL signal. This light was delivered, through a microscope objective, by a fibered laser diode at 660 nm, using its highest power of 51 mW. The external X-ray beam was delivered by the MOPERIX facility of Laboratoire Hubert

Curien. The machine has been operated at 100 kV and a current of 45 mA, generating photons of ~40 keV average energy. The dose-rates at the various locations have been measured with an ionization chamber. All the values of dose rate and doses have been converted by taking into account the ratio Z_{eff}(water)/Z_{eff}(silica). Doses are consequently given in Gy(silica) unit.

For the RL measurements, the same setup has been used except that the spectral filter was removed and the laser diode was switched-off. Indeed, this readout mode consists in measuring the emission signal directly during the irradiation, with no need of a stimulated light to de-trap the charges. Photoluminescence spectra were recorded at room temperature by exciting the samples with the 351 nm line of an argon laser with a power of 5 mW. The emitted light was imaged onto the slit of a Jobin-Yvon U1000 monochromator and collected using a Hamamatsu R943-02 photomultiplier tube.

RL spectrum was recorded by using a QE Pro spectrometer (Ocean optics). The dark signal has been systematically subtracted from the RL spectra.

III. Experimental Results

A. *Glass structure*

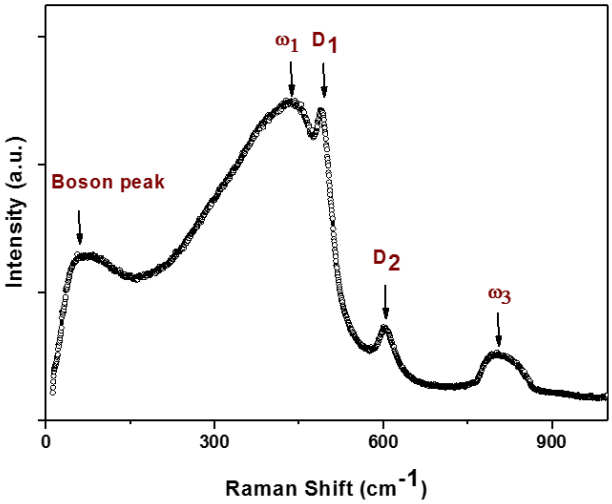

Fig.2: Raman spectrum of a Ce doped SiO_2 rod.

Fig.2 shows the Raman spectrum of the Ce-doped SiO_2 rod. It presents the well-known bands of SiO_2 glass. In the low-frequency region, the "Boson peak", which characterizes the vitreous state, is seen around 56 cm^{-1}. The large band centered around 440 cm^{-1} is assigned to the Si-O-Si network deformation vibration (ω_1). As well, the asymmetric band located around 810 cm^{-1} (ω_3) is attributed to a complex vibration involving substantial silicon motion in addition to a bending movement of oxygen in a vitreous network. The two smaller bands at 490 cm^{-1} (D_1) and 603 cm^{-1} (D_2) are assigned to symmetric stretching modes of three- and four-member siloxane rings, respectively, in the silica network [33].

B. *Radioluminescence*

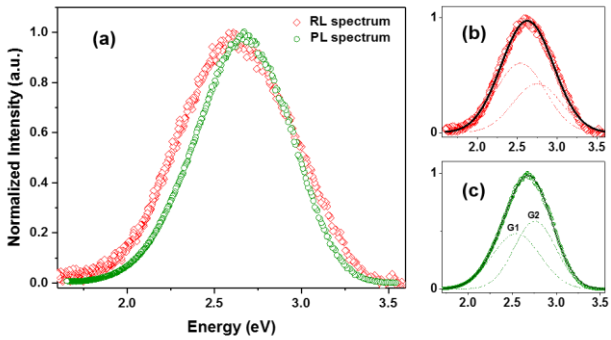

Fig.3: (a) Normalized RL and PL (under laser excitation at 351 nm) spectra of a Ce-doped silica rod. (b) and (c) present the decomposition of the RL and PL spectra, respectively, into two Gaussian components G1 and G2.

Fig.3 presents the emission spectrum under X-ray (RL) and the photoluminescence spectrum under 351 nm laser excitation. RL and PL spectra exhibit a band peaking around 2.62 eV (473 nm) and 2.67 eV (464 nm) with full widths at half maximum of 0.77 eV and 0.65 eV respectively. This band is clearly asymmetrical. It is attributed to the allowed electric dipole 5d-4f transition of Ce^{3+} [34] and can be decomposed into two Gaussian components (G1 and G2), with energy positions of 2.54 and 2.75 eV, respectively. These two values are ascribed to the splitting of the ground level 4f into two sublevels by spin-orbit interaction [28]. The splitting effect, which is independent of the excitation (UV or X-ray), is however weaker than that mentioned in reference [28]. On the other hand, the slight energy shift between both spectra (RL and PL) can be attributed to the different characteristics of the Gaussian components G1 and G2. In effect, the values of the ratio between the sub-band areas G1/G2 are 1.45 and 0.94 for RL and PL spectra, respectively. This result could be related to the different excitation-emission mechanisms in PL and RL processes. In the PL case, the cerium ions are immediately excited by incident photon energy. In the case of RL, X-ray irradiation firstly generates electron-hole pairs, which then relax through defect traps before the final radiative recombination on the excited centers. As a result, the sub-levels G1 and G2 are not filled in the same way.

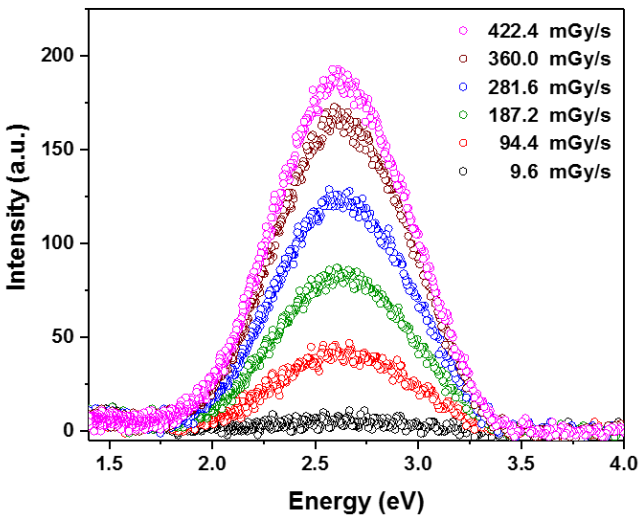

Fig.4: X-ray RL spectra obtained under different dose rates.

In Fig. 4 are reported the RL spectra of the Ce-doped rod under X-ray irradiations for various dose rates. As expected, the integrated area of RL band increases with the dose rate. Fig.5 shows the dependence of the integrated RL intensity (determined from Fig.4) on the dose rate. This figure reveals the linear behavior of the signal in the investigated dose rate range, namely up to at least 420 mGy/s (SiO_2).

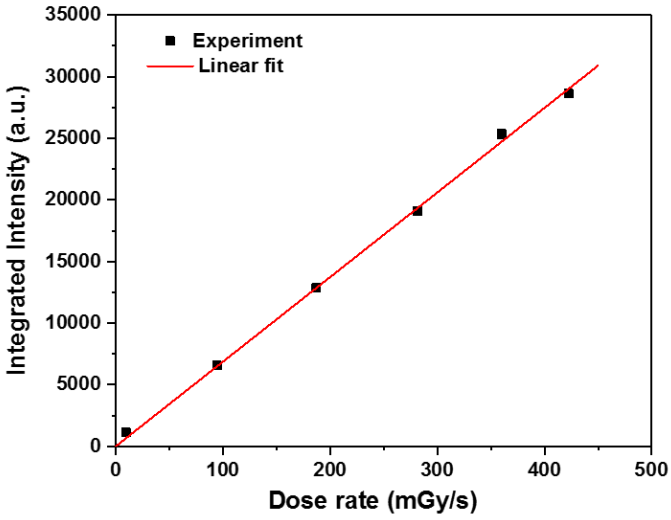

Fig.5: Integrated RL intensity plotted against dose rate for the Ce-doped rod.

Fig.6 (a) shows the typical dynamics of the RL signal intensity collected by the PMT under a dose rate of 251 mGy/s, where the background noise, measured in the dark without excitation, has been subtracted. This response shows a high reproducibility: repeating the measurements several times led to variations of less than 1% of the mean voltage. As the X irradiations starts, the RL signal first increases for a few seconds, to finally tend toward a plateau.

This delayed response of the material to irradiation is due to carrier trap states. Indeed, during the irradiation, the prompt recombination causing the production of the RL signal is in competition with electron trapping. However, while the electron traps, including shallow and deep ones, are filled, the trapping probability decreases and then, more electrons become available for recombination. The RL signal rises to a steady-state level, which increases for each increasing dose rate. Such an effect is detrimental to the use of the scintillating materials in real-time dose monitoring. In this respect, our Ce-doped silica rod has a much faster response than that of Al_2O_3:C, for example, which presents deep trap levels and thus takes longer time to reach saturation [35]-[37].

Fig.6 (b) illustrates the linear dose rate dependence of the RL signal measured with the PMT in the explored range between 26 and 1187 mGy/s. This result is very promising since the reproducibility of this trend is quite good and the linearity range is larger than the one reported with other Ce-doped silica fibers. For example, a linear dependence of the RL intensity versus the dose rate has been found for a Ce^{3+}-doped SiO_2 fiber under X-rays photons up to 40 mGy/s [34].

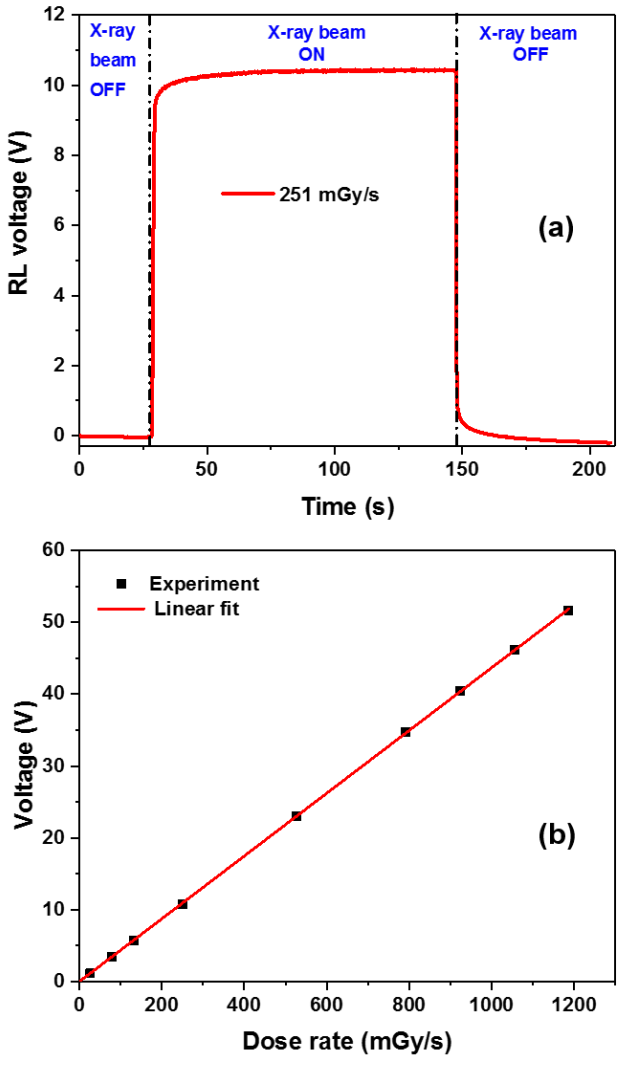

Fig.6: a) the RL signal under X-rays for a dose rate of 251 mGy/s. b) Dose response of the Ce-doped rod. The data points present the RL signal taken on the plateau after a background subtraction.

C. Dose dependence of the OSL signal

When the rod is exposed to radiation, free electrons and holes are created but some of them are then trapped at metastable energy levels in the bandgap between the conduction band and the valence one. These energy levels are attributed either to intrinsic defects of the silica matrix or to the doping ions. When the irradiation is stopped, the glass can be illuminated using the laser diode through the dedicated optical fiber, so as to release the trapped electrons that are stimulated into the conduction band. Those freed electrons are then allowed to recombine with holes at the recombination centers to generate the OSL signal [35]. It is known from the literature that the Ce^{3+} behaves as a recombination center for carriers created during irradiation [38].

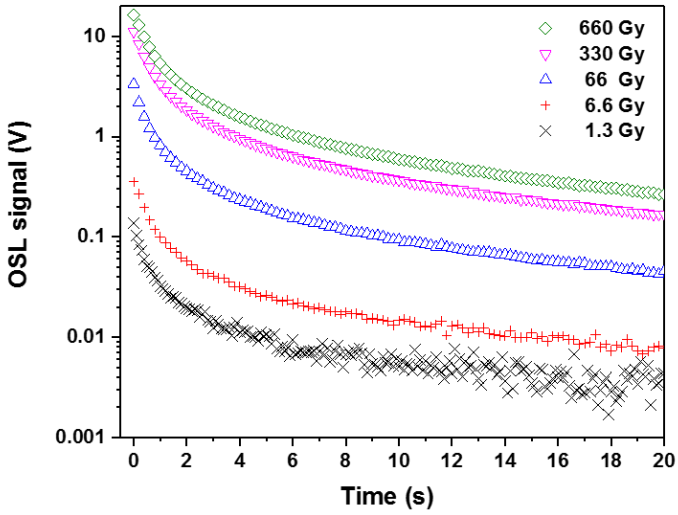

Fig. 7: OSL decay curves for different X-ray exposure times at a dose rate of 660 mGy/s (in silica) after stimulation with a probe laser at λ = 660 nm.

Fig. 7 presents the OSL decay curves of the Ce-doped sample under stimulation at 660 nm, recorded immediately (2 s) after radiation exposure at a dose rate of 660 mGy/s (SiO_2) for different durations. Fig.8 illustrates the integral OSL signal versus accumulated X-ray dose, for doses ranging between 3.5 Gy and 2765 Gy (SiO_2).

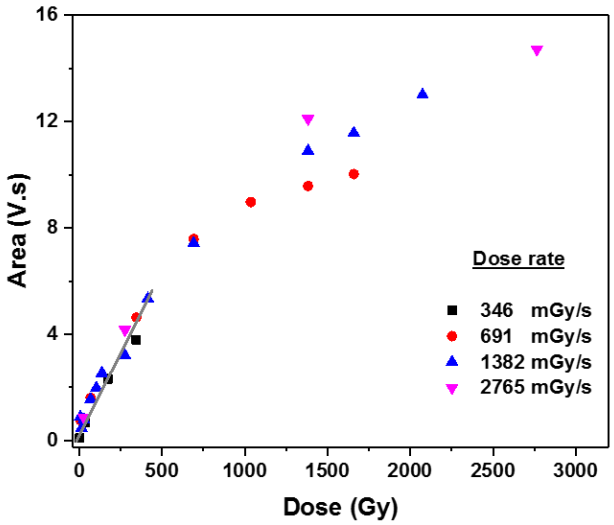

Fig. 8: Dose response of the OSL signal obtained with different dose rates. Each point represents the total integrated response under stimulation and after X-ray irradiations of Ce-doped sample.

To analyze this response, the decaying OSL curve was integrated over the whole time interval until the stabilization of the signal, after having subtracted the noise background and the offset due to the stimulating laser. Thus, this time interval was long enough to deplete the trap concentrations to zero. As a result, this interval depended on the given dose since the asymptotic behavior of the signal is attained at different times according to the deposited dose. In Fig. 8, a linear dependence of the OSL signal with X-ray dose is confirmed up to 500 Gy, independently of the dose rate. For doses higher than 500 Gy, the OSL signal reaches a nonlinear behavior but does not completely saturate up to 2.7 kGy. Moreover, in the non-linear zone corresponding to the highest doses, the response seems to depend on the dose rate. Indeed, for a given accumulated dose, the lower the dose rate, the lower the OSL signal. This result is consistent with the thermal fading of the signal (Fig. 10: see section E) since during long irradiation time, both filling of the traps and fading are taking place simultaneously [39].

D. OSL Kinetics

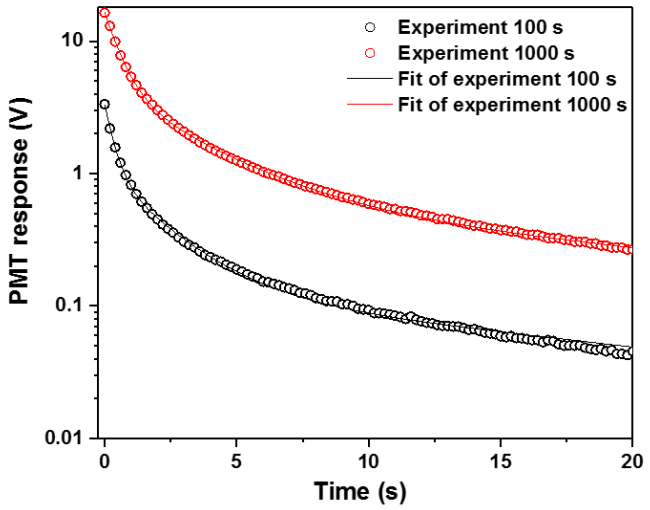

Fig.9: OSL decay curves after X-ray exposures at 66 Gy and 660 Gy (SiO_2), at a dose rate of 660 mGy/s, with their corresponding 3-exponential function fits.

Fig. 9 shows the OSL decay profiles of the Ce-doped rod after two different exposure times at a dose rate of 660 mGy/s. OSL decay curves after X-ray irradiation at all deposited doses are well approximated by a sum of three exponential decay functions:

$$I = A_f\, e^{-t/\tau_s} + A_m\, e^{-t/\tau_m} + A_s\, e^{-t/\tau_f} \qquad (1)$$

where A_f (τ_f), A_m (τ_m) and A_s (τ_s) are the amplitudes (decay times) of the fast, medium and slow components respectively. Two possible interpretations may be given for the existence of those three contributions to the OSL decay [40]. The first one involves a single trap with a single "bleachability" (rate of charge release), but including significant retrapping, so that the OSL decay cannot be fitted by a single exponential function. The second admitted interpretation considers that OSL decay results from the release of charges from several trap levels having different thermal activation energies and considering that retrapping phenomenon is minor.

In our case, the derived decay times are summarized in Table 1 for the linear domain (100 s; 66 Gy) and in the saturation regime (1000 s; 660 Gy). In Table 1, the shortest and intermediate time constants obtained from this fit significantly increase with the deposited dose, on the contrary of the longest time constant that remains of the same order. Nevertheless, the decay times globally increase with the accumulated dose. This result could be related to retrapping phenomena during the longer irradiation time duration required to reach the highest dose. However, at this stage, we cannot absolutely attribute each decay time to one specific and defined kind of trap. This will need complementary experimental results (such as TL) and a thorough theoretical study.

TABLE I
The different decay times of the OSL signal for different doses.

		Fast	Medium	Slow
66 Gy	**τ (s)**	0.3	2.0	19.5
	Contribution (%)	69	27	4
660 Gy	**τ (s)**	0.6	3.1	21.9
	Contribution (%)	73	23	4

E. Fading of the OSL Signal

One of the major and important criteria for dosimetry is the stability of the measured OSL signal with time. In many cases and at ambient temperature, trapped carriers can be thermally released from defect traps to undergo recombination, thus reducing the anticipated signal which is related to the number of trapped carriers. The elapsed time between the end of the excitation by the ionizing radiation and the readout has an effect on the measured signal [41, 42]. This phenomenon has been reported by a number of authors and in several materials.

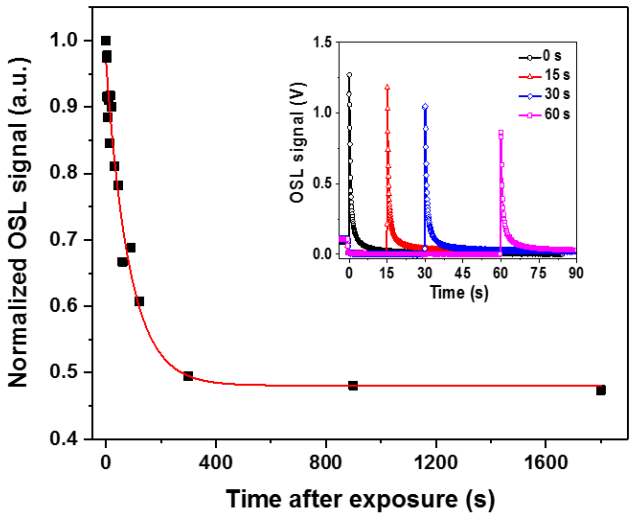

Fig.10: Fading response of the integrated OSL signal for an accumulated dose of 26.4 Gy

Fig.10 presents an example of this fading phenomenon of the OSL signal for an accumulated dose of 26.4 Gy, where data are normalized to the response obtained directly after the end of the exposure to radiation at ambient temperature. As can be seen, a signal loss of about 53 % occurs in six minutes. After that time, the signal remains stable, which means that the spontaneous depopulation of the trapped levels seems to be completed. Hence, it can be argued that our Ce-doped silica undergoes a rather strong but "short-time" fading, as compared to other OSL materials. Indeed, for example, $CaSO_4$:Eu showed a 10 % fading after 24 hours and after that, negligible further changes were observed [43]. Also, it was shown that in a cerium doped lutetium orthosilicates crystal films, 85 % of the initial OSL signal remains after 18 h [41]. Moreover, non-significant fading (1.8 % after three weeks) was observed in an Al_2O_3:C films for dosimetry in therapeutic photon and electron beams [42]. Although in all these previous works, a limited fading seemed

to be observed, it consisted in a "long-time" fading. In each case, the authors did not clarify if they observed a short-time fading and the starting delay for the measurement of this fading after the end of irradiation. To the best of our knowledge, the present paper is the first one to investigate thermal fading phenomena in both short-time and intermediate-time scales using a fibered setup. Long term fading will be investigated in future works in order to understand the stability of the optical material response.

IV. Conclusion

In this work, we have firstly shown that the RL of the studied sol-gel Ce-doped silica glass presents a linear response up to dose rates of 1.2 Gy/s at least. Secondly, the OSL signal is also characterized by a linear response up to 500 Gy, which makes these Ce-doped materials very promising for dosimetry in harsh environment, even in the case of high dose rate conditions. Moreover, the OSL decay curve has been fitted by a sum of three exponential decay functions and the corresponding decay times globally increase with the accumulated dose. Finally, fading phenomenon strongly occurs during the first minutes after irradiation, reducing the OSL signal by 50%, then this signal remains stable.

ACKNOWLEDGMENT

This work was partially supported by IRCICA institute (www.ircica.univ-lille1.fr) and CERLA platform of University of Lille.

References

[1] A. K. M. Mizanur Rahman, H. T. Zubair, M. Begum, H. A. Abdul-Rashid, Z. Yusoff, N. M. Ung, K. A. Mat-Sharif, W. S. Wan Abdullah, G. A. Mahdiraji, Y. M. Amin, M. J. Maah, and D. A. Bradley, "Germanium-doped optical fiber for real-time radiation dosimetry", *Rad. Phys. Chem.*, vol. 116, pp. 170-175, Nov. 2015.

[2] B. L. Justus, P. Falkenstein, A. L. Huston, M .C. Plazas, H. Ning, and R. W. Miller, "Gated fiber-optic-coupled detector for in vivo real-time radiation dosimetry", *Appl. Opt.* vol. 43, no. 8, pp. 1663-1668, Mar. 2004.

[3] A. Berra, V. Conti, D. Lietti, L. Milan, C. Novati, A. Ostinelli, M. Prest, C. Romanó, and E. Vallazza, "A SiPM based real time dosimeter for radiotherapic beams", *Nucl. Instrum. Methods Phys. Res. Sect. A*, vol. 773, pp. 72-80, 2015.

[4] E. G. Yukihara and S. W. S. McKeever, "Optically stimulated luminescence: fundamentals and applications", Wiley & Sons, 2011.

[5] P. Woulfe, F. J. Sullivan and S. O'Keeffe, "Optical fibre luminescence sensor for real-time LDR brachytherapy dosimetry", *Proc. SPIE*, vol. *9916*, pp. 99160T-1–99160T-4, 2016.

[6] S. O'Keeffe et al., "An Optical Fibre-Based Sensor for Real-Time Monitoring of Clinical Linear Accelerator Radiotherapy Delivery", *IEEE J. Sel. Topics Quantum Electron.*, vol. 22, no. 3, pp. 35-42, May/Jun. 2016.

[7] P. Ferdinand, S. Magne and G. Laffont, "Optical fiber sensors to improve the safety of nuclear power plants", *Proc. SPIE*, vol. 8924, pp. 89242G, 2013.

[8] P. D. Sahare, "High-Energy Radiation Dosimetry in the Space", *J. Astrophys. Aerospace Technol*., vol. 2, no. 1, pp. 1000e105-1–1000e105-2, 2012.

[9] S. W. S. McKeever, "New millennium frontiers of luminescence dosimetry", *Radiat. Prot. Dosim.*, vol. 100, no. 1-4, pp. 27-32, Jul. 2002.

[10] L. Dusseau , D. Plattard, J. R. Vaillé, G. Polge, G. Ranchoux, F. Saigné, J. Fesquet, R. Ecoffet, and J. Gasiot, "An Integrated Sensor Using Optically Stimulated Luminescence for In-Flight Dosimetry", *IEEE Trans. Nucl. Sci.*, vol. 47, no. 6, pp. 2412-2416, Dec. 2000.

[11] D. Plattard, G. Ranchoux, L. Dusseau, G. Polge, J.-R. Vaillé, J. Gasiot, J. Fesquet, R. Ecoffet, and N. Iborra-Brassart, "Characterization of an Integrated Sensor Using Optically Stimulated Luminescence for In-Flight Dosimetry", *IEEE Trans. Nucl. Sci.*, vol. 49, no. 3, pp. 1322- 1326, Jun. 2002.

[12] J. C. Polf, S. W. S. McKeever, M. S. Akselrod, and S. Holmstrom, "A real-time, fibre optic dosimetry system using Al_2O_3 fibres", *Radiat. Prot. Dosim.*, vol. 100, no. 1-4, pp. 301-304, Jul. 2002.

[13] R. Gaza, S. W .S. McKeever, M. S. Akselrod, A. Akselrod, T. Underwood, C. Yoder, C. E. Andersen, M. C. Aznar, C. J. Marckmann and L. Bøtter-Jensen, "A fiber-dosimetry method based on OSL from Al_2O_3:C for radiotherapy applications", *Radiat. Meas.*, vol. 38, no. 4-6, pp. 809-812, Aug./Dec. 2004.

[14] D. M. Klein, A. C. Lucas and S. W. S. McKeever, "A low-level environmental radiation monitor using optically stimulated luminescence from Al_2O_3:C: Tests using ^{226}Ra and ^{232}Th sources", *Radiat. Meas.*, vol. 46, no. 12, pp. 1851-1855, Dec. 2011.

[15] D. M. Klein, S. W. S. McKeever, "Optically stimulated luminescence from KBr:Eu as a near-real-time dosimetry system", *Radiat. Meas.*, vol. 43, no. 2-6, pp. 883-887, Feb./Jun. 2008.

[16] R. Gaza and S. W. McKeever, "A real-time, high-resolution optical fibre dosemeter based on optically stimulated luminescence (OSL) of KBr:Eu, for potential use during the radiotherapy of cancer", *Radiat. Prot. Dosim.*, vol. 120, no. 1-4, pp. 14-19, Sep. 2006.

[17] A. Twardak, P. Bilski, Y. Zorenko, V. Gorbenko and O. Sidletskiy, "OSL dosimetric properties of cerium doped lutetium orthosilicates", *Radiat. Meas.*, vol. 71, pp. 139-142, Dec. 2014.

[18] C. B. Palan, K. A. Koparkar, N. S. Bajaj and S. K. Omanwar, "Synthesis and TL/OSL properties of $CaSiO_3$:Ce biomaterial", *Mater. Lett.*, vol. 175, pp. 288-290, Jul. 2016.

[19] Y. Fujimoto, T. Yanagida, Y. Futami and H. Masai, "Fluorescence and radiation response properties of Ce^{3+}-doped $CaO–Al_2O_3–B_2O_3$ glass", *Japan. J. Appl. Phys.*, vol. 53, no. 5S1, pp. 05FK05-1–05FK05-3, Apr. 2014.

[20] H. El Hamzaoui, B. Capoen, N. Al Helou, G. Bouwmans, Y. Ouerdane, A. Boukenter, S. Girard, C. Marcandella, O. Duhamel, G. Chadeyron, R. Mahiou and M. Bouazaoui, "Cerium-activated sol-gel silica glasses for radiation dosimetry in harsh environment", *Mater. Res. Express*, vol. 3, no. 4, pp. 046201-1–046201-7, 2016.

[21] W. Chewpraditkul, Y. Shen, D. Chen, B. Yu, P. Prusa, M. Nikl, A. Beitlerova and C. Wanarak, "Luminescence and scintillation of Ce^{3+}-doped high silica glass", *Opt. Mater.*, vol. 34, no. 11, pp. 1762-1766, Sep. 2012.

[22] C. Jiang, P. Deng, J. Zhang and F. Gan, "Radioluminescence of Ce^{3+}-doped $B_2O_3–SiO_2–Gd_2O_3–BaO$ glass", *Phys. Lett. A*, vol. 323, no. 3-4, pp. 323-328, Mar. 2004.

[23] J. Qiu, N. Sugimoto, Y. Iwabuchi and K. Hirao, "Photostimulated luminescence in Ce^{3+} doped silicate glasses", *J. Non-Cryst. Solids*, vol. 209, no. 1-2, pp. 200-203, Jan. 1997.

[24] T. Yanagida, J. Ueda, H. Masai, Y. Fujimoto and S. Tanabe, "Optical and scintillation properties of Ce-doped $34Li_2O–5MgO–10Al_2O_3–51SiO_2$ glass", *J. Non-Cryst. Solids*, vol. 431, pp. 140-144, Jan. 2016.

[25] Y. Yao, L. Liu, Y. Zhang, D .Chen, Y. Fang and G. Zhao, "Optical properties of Ce^{3+} doped fluorophosphates scintillation glasses", *Opt. Mater.*, vol. 51, pp. 94-97, Jan. 2016.

[26] L. Liu, C. Shao, Y. Zhang, X. Liao, Q. Yang, L. Hu and D. Chen, "Scintillation properties and X-ray irradiation hardness of Ce^{3+}-doped Gd_2O_3-based scintillation glass", *J. Lumin.*, vol. 176, pp. 1-5, Aug. 2016.

[27] J. M. Ogiegło, A. Zych, Konstantin V. Ivanovskikh, T. Jüstel, C. R. Ronda and A. Meijerink, "Luminescence and energy transfer in $Lu_3Al_5O_{12}$ scintillators co-doped with Ce^{3+} and Tb^{3+}", *J. Phys. Chem. A*, vol. 116, no. 33, pp. 8464-847, 2012.

[28] M. Fasoli, A. Vedda, A. Lauria, F. Moretti, E. Rizzelli, N. Chiodini, F. Meinardi and M. Nikl, "Effect of reducing sintering atmosphere on Ce-doped sol–gel silica glasses", *J. Non-Cryst. Solids*, vol. 355, no. 18-21, pp. 1140-1144, Jul. 2009.

[29] M. Carrara, C. Cavatorta, M. Borroni, C. Tenconi, A. Cerrotta, C. Fallai, G. Gambarini, A. Vedda and E. Pignoli, "Characterization of a Ce^{3+} doped SiO_2 optical dosimeter for dose measurements in HDR brachytherapy", *Radiat. Meas.*, vol. 56, pp. 312-315, Sep. 2013.

[30] N. Chiodini, A. Vedda, M. Fasoli, F. Moretti, A. Lauria, M. C. Cantone, I. Veronese, G. Tosi, M. Brambilla, B. Cannillo, E.Mones, G. Brambilla and M. Petrovich, "Ce-doped SiO_2 optical fibers for remote radiation sensing and measurement", *Proc. SPIE*, vol. 7316, pp. 731616-1–731616-8, 2009.

[31] G. Okada, S. Kasap and T. Yanagida, "Optically- and thermally-stimulated luminescences of Ce-doped SiO_2 glasses prepared by spark plasma sintering", *Opt. Mater.*, vol. 61, pp. 15-20, Nov. 2016.

[32] H. El Hamzaoui, L. Courtheoux, V. Nguyen, E. Berrier, A. Favre, L. Bigot, M. Bouazaoui, and B. Capoen, "From porous silica xerogels to bulk optical glasses: The control of densification", *Mater. Chem. Phys.* vol. 121, no. 1-2, pp. 83-88, May 2010.

[33] N. Al Helou, H. El Hamzaoui, B. Capoen, Y. Ouerdane, A. Boukenter, S. Girard, M. Bouazaoui, "Effects of ionizing radiations on the optical properties of ionic copper-activated sol-gel silica glasses", *Opt. Mater.*, vol. 75, pp. 116-121, Jan. 2018.

[34] A. Vedda, N. Chiodini, D. Di Martino, M. Fasoli, S. Keffer, A. Lauria, M. Martini, F. Moretti, and G. Spinolo, "Ce^{3+}-doped fibers for remote radiation dosimetry" , *Appl. Phys. Lett*., vol. 85, no. 26, pp. 6356, 2004.

[35] J.C. Polf, E.G. Yukihara, M.S. Akselrod, S.W.S. McKeever, "Real-time luminescence from Al_2O_3 fiber dosimeters", *Radiat. Meas*., vol. 38, no. 2, pp. 227-240, Apr. 2004.

[36] M. Aznar, "Real-time in vivo luminescence dosimetry in radiotherapy and mammography using Al_2O_3:C." Ph.D. dissertation, Risø-PhD-12(EN), Risø National Laboratory, Denmark, 2005.

[37] C.E. Andersen, S.K. Nielsen, S. Greilich, J. Helt-Hansen, J. C. Lindegaard and K. Tanderup, "Characterization of a fiber-coupled Al_2O_3:C luminescence dosimetry system for online in vivo dose verification during ^{192}Ir brachytherapy", *Med. Phys.*, vol. 36, no. 3, pp. 708-718, Mar. 2009.

[38] F. Moretti, G. Patton, A. Belsky, M. Fasoli, A. Vedda, M. Trevisani, M. Bettinelli, and C. Dujardin, "Radioluminescence Sensitization in Scintillators and Phosphors: Trap Engineering and Modeling", *J. Phys. Chem. C* , vol. *118* , no. 18, pp.9670-9676, Apr. 2014.

[39] R. Chen, V. Pagonis and J.L. Lawless, "Time and dose-rate dependence of TL and OSL due to competition between excitation and fading", *Radiat. Meas*., vol. 82, pp. 115-121, Nov. 2015.

[40] R. M. Bailey, B. W. Smith and E. J. Rhodes, "Partial bleaching and the decay form characteristics of quartz OSL", *Radiat. Meas.*, vol. 27, no. 2, pp. 123-136, Apr. 1997.

[41] A. Twardak, P. Bilski, Y. Zorenko, V. Gorbenko, O. Sidletskiy, "OSL dosimetric properties of cerium doped lutetium orthosilicates", *Radiat. Meas*., vol. 71, pp. 139-142, Dec. 2014.

[42] V.Schembri, and B. J. M. Heijmen, "Optically stimulated luminescence (OSL) of carbon-doped aluminum oxide Al_2O_3: C for film dosimetry in radiotherapy", *Med. Phys*., vol. 34, no. 6, pp. 2113-2118, Jun. 2007.

[43] M. S. Kulkarni, R R. Patil, A. Patle, N. S. Rawat, P. Ratna, B. C. Bhatt, S. V. Moharil, "Optically stimulated luminescence from $CaSO_4$:Eu-Preliminary results", *Radiat. Meas*., vol. 71, pp. 95-98, Dec. 2014.